

Mid-latitude Temperatures at 87 km: Results From Multi-instrument Fourier Analysis

Douglas P. Drob¹, J. Michael Picone¹, Stephen D. Eckermann¹, C. Y. She², J. F. Kafkalidis³, D. A. Ortland^{3,4}, R. J. Niciejewski³, and T. L. Killeen³

Abstract. Using a novel Fourier fitting method we combine two years of mid-latitude temperature measurements at 87 km from the High Resolution Doppler Imager, the Colorado State University lidar, and the Peach Mountain Interferometer. After accounting for calibration bias, significant local-time variations on the order of 10 K were observed. Stationary planetary waves with amplitudes up to 10 K were observed during winter, with weaker wave amplitudes occurring during other seasons. Because of calibration biases among these instruments, we could estimate the annual mean temperature to no better than 193.5 ± 8.5 K.

1. Introduction

State parameters in the mesosphere and lower thermosphere (henceforth MLT) are difficult to estimate because significant observational aliasing can occur due to irregular and incomplete sampling of the region in space and time [Salby, 1982; Forbes *et al.*, 1997]. These problems are compounded by the possibility of direct observational biases specific to a given measurement technique. While advanced data assimilation methods and sufficient data exist for tropospheric and stratospheric objective analysis, MLT temperature data and dynamical models are currently inadequate to employ such techniques. Two notable attempts, however, to combine multi-instrument satellite and ground-based MLT data to specify the spatiotemporal variability of the region are the MSISE-90 empirical model of Hedin [1991] and recent work by Leblanc *et al.* [1999]. We present a methodology for making statistical estimates of mid-latitude temperature fields using a combination of satellite and ground-based data. Results at a height of 87 km are presented here to illustrate the method and its potential future use with larger multi-instrument data sets.

Figure 1a shows the combined longitudinal and temporal sampling pattern of the temperature field between $41^\circ \pm 1^\circ$ N at 87 km over a two-year period from the High Resolution Doppler Interferometer (HRDI) [Ortland *et al.*, 1998], the Colorado State University (CSU) lidar [She and von Zahn, 1998], and the Peach Mountain Interferometer (PMI) [Niciejewski and Killeen, 1995]. The CSU lidar and PMI are located at 40.6° N, 105° W and 41° N, 83° W, respectively. The OH(3-1) rotational temperatures measured by the PMI are assumed to originate from a layer at 87 ± 4 km [She and Lowe, 1998]. Additional information on the mean altitude of the OH nightglow layer and its spatiotem-

poral variability is provided by Yee *et al.* [1997] and Melo *et al.* [1999]. In this study we have used HRDI level 3AT version 11 data which have a vertical resolution of 3 km.

Figure 1b shows the corresponding sampling patterns as a function of day number and local time. Gaps are due to the HRDI yaw cycle, cloud cover, and instrument downtime. The HRDI observations are daytime measurements, while the ground-based observations are performed at night. Figure 1b illustrates the asynchronous sampling pattern of the HRDI instrument, which precesses through all local times in 36 days. Note from Figure 1 that combining data from all three instruments significantly improves the spatial and temporal data coverage compared to consideration of data from a single instrument.

2. Methodology

Next we seek to combine these data to make a detailed estimate of mid-latitude temperature variability at 87 km. As a prototype we have used non-sequential, error-weighted, least-squares estimation without dynamical constraints. The idea is to perform simultaneously two Fourier harmonic surface fits of the space-time distribution of measurements (Figure 1a) and the time-time distribution (Figure 1b). The inversion method combines space-time analysis to capture the quasi-stationary planetary wave field [e.g. Salby, 1982] with non-linear time series analysis to capture the migrating tidal field, while accounting for seasonal changes in the mean. An important zeroth-order correction term is also included to account for possible instrument biases. The multi-dimensional Fourier model is:

$$\Psi(t, \lambda, \tau) = \sum_{n=0}^N \sum_{s=-S, s \neq 0}^S [a_{ns} \cos(\kappa_s \lambda + \sigma_n t) + b_{ns} \sin(\kappa_s \lambda + \sigma_n t)] + \sum_{n=0}^N \sum_{m=-M, m \neq 0}^M [c_{nm} \cos(\omega_m \tau + \sigma_n t) + d_{nm} \sin(\omega_m \tau + \sigma_n t)] + \sum_{n=0}^N [e_n \cos(\sigma_n t) + f_n \sin(\sigma_n t)] + \sum_{k=1}^K \beta_k \alpha_k \quad (1)$$

The first Fourier expansion is a space-time model, where t is time in days, λ is longitude and a_{ns} and b_{ns} are real Fourier coefficients. This term represents the inter-seasonal variations in the longitudinal structure of quasi-stationary planetary waves. The spatial and temporal frequencies are $\kappa_s = s2\pi/360^\circ$ and $\sigma_n = n2\pi/\Delta T_n$ with s and n as the respective integer harmonics. The windowing period ΔT_n and total orders N , M , and S can be chosen to suit the task at hand. In the second Fourier expansion, τ is local time in hours, c_{nm} and d_{nm} are real Fourier coefficients for integer harmonics n and m , respectively, and $\omega_m = m2\pi/\Delta T_m$. This term represents the seasonal amplitude and phase modulations of the fundamental westward propagating tidal harmonics, i.e. the diurnal (1,1) and semi-diurnal (2,2) modes.

¹Naval Research Laboratory, Washington DC

²Colorado State University, Fort Collins, Colorado

³University of Michigan, Ann Arbor, Michigan

⁴NorthWest Research Associates, Bellevue, Washington

Copyright 2000 by the American Geophysical Union.

Paper number 1999GL010821.
0094-8276/00/1999GL010821\$05.00

The third term in (1) represents the seasonal variation of the zonal mean, which has been separated from the first two terms to avoid redundant harmonics. The last term is introduced to account for zeroth order instrument calibration biases, where α_k is an indicator function which takes the value of unity for an observation from the k^{th} instrument (otherwise it is zero). It is used to tag observations from the k^{th} instrument for multiplication by the bias correction factor β_k in a matrix formulation of the forward model.

With a total of J measurements from K instruments the $2S + 2NS + 2M + 2NM + 2N + K$ unknown coefficients ($a_{ns}, b_{ns}, c_{nm}, d_{nm}, e_n, f_n, \beta_k$) can be estimated in an error-weighted, least-squares sense from the overdetermined system of J linear equations using Singular Value Decomposition (SVD) inverse methods [Wunsch, 1996]. Because all harmonic components are estimated simultaneously and are resolved by the data (see Figure 1), aliasing among the mean, quasi-stationary planetary waves, and tidal components is effectively eliminated.

In constructing this model we have assumed that the relative variations within a given data subset are unbiased, but that time-independent calibration biases are possible in each data set. The coefficients β_k represent the average departure of observations from the k^{th} instrument from some annual mean. To facilitate this formulation the annual mean temperature (estimated here as the sample mean of the entire data set) is subtracted from the data before fitting. Analysis performed using synthetic data indicates that adequate information exists in the data to resolve both the diurnal harmonic and the bias terms, despite the functional similarities. If time-dependent instrument biases exist in the data (for example from seasonal changes in the height of the OH nightglow layer) the corresponding effect on the state estimates will be weighted inversely by the statistical uncertainties of the data and proportionately by the relative influence of the data subset on each model parameter. In future analyses of upper-atmospheric data sets, valuable insight into time-dependent observational biases can be obtained by application of (1) followed by a statistical analysis of the solution residuals.

A number of choices of $N, S, M, \Delta T_n$, and ΔT_m are possible. We show results for the current data set using $N = 5, M = 3, S = 5, \Delta T_n = 730$ days, and $\Delta T_m = 24$ hours. In the current inversion the solution at the endpoints is forced to be periodic so that the estimates for January 1, 1993 and December 31, 1994 will be similar. Over the two-year period there were $J = 12685$ observations; 7672 observations at 87 km between 40° and 42° N made by HRDI, 2496 hourly-averaged measurements between 86.0 and 88.0 km made by the CSU lidar (3×832), and 2517 hourly-averaged measurements made by the PMI. In order to account properly for geophysical variability from gravity waves that is not captured by (1) and more evenly weight the three data sets, the reported measurement uncertainties were adjusted to reflect the magnitude of geophysical root mean square temperature fluctuations. While maintaining the relative variations within each data set the reported uncertainties were renormalized to a mean value of 7 K.

3. Results

The sample means and standard deviations of the individual data sets over the two year period are 186.6 ± 15.2 K (HRDI), 203.4 ± 18.8 K (CSU) and 205.8 ± 22.1 K (PMI).

Differences in these means can be interpreted as day-to-night temperature changes, instrument bias effects, or a combination of both. If geophysical effects caused these differences, the mean diurnal amplitude over a two-year period would have to be greater than 10 K with minima occurring near local noon. Recently *States and Gardner* [1998, 2000b] observed diurnal amplitudes of this order at these altitudes during most seasons but with temperature maxima occurring at local noon. Climatological comparisons of data from ground-based lidars and daytime Solar Mesosphere Explorer (SME) observations by *Clancy et al.* [1994] also show that, on average, mid-latitude temperatures are warmer during daytime at 87 km. In addition, discontinuous jumps in the monthly average local time behavior of the three data sets are observed at sunrise and sunset. By adding bias correction terms to the inversion, the global mean of each data set is self-consistently adjusted so that the local time behavior is continuous at the dawn/dusk boundaries between data sets.

Figure 2 shows the seasonal evolution of the diurnal harmonic estimated with and without a bias correction term in (1). The results obtained without a bias correction (Fig. 2a) indicate a diurnal harmonic as large as 15 K, with near constant phase maxima at night. The results obtained with the bias correction term (Fig. 2b) indicate phase maxima occurring mostly during the day, supporting the conclusions of *States and Gardner* [1998, 2000b] and *Clancy et al.* [1994]. In addition the winter pre-dawn temperature enhancement in Figure 2b is also observed by *States and Gardner* [2000b]. This is thought to be the effect of in-situ chemical heating from the $H+O_3$ reaction which peaks in winter at night-time at 87 km [*Mlynczak et al.*, 1991]. We also note that with or without a bias term, our estimates of the seasonal evolution of the semidiurnal tidal amplitudes and phases are generally consistent with other estimates in the literature [*Williams et al.*, 1998; *States and Gardner*, 2000b].

The derived systematic bias correction factors defined in (1) are -7.2 ± 3.4 K (HRDI), 8.7 ± 4.7 K (CSU) and 10.5 ± 4.7 K (PMI). In reporting these values we have assumed that systematic biases are equally probable in each measurement technique. The sample mean and standard deviation of the total data set is 195.3 K and 19.7 K, respectively. Based on the magnitudes of instrument biases, the systematic uncertainty in the annual mean temperature at 87 km over this period is approximately ± 8.5 K. Thus, by a statistical consensus of currently available data the magnitude of the mid-latitude annual mean temperature at mesopause altitudes is uncertain.

Figure 3 shows the total day-of-year/local-time temperature estimates at 87 km at 0° E (Figure 3a) and 180° E (Figure 3b). These fields have been reconstructed using the estimated Fourier coefficients in (1). The error-propagated uncertainties of the individual harmonic components are on the order of ± 3 K. On comparing Figure 3a and Figure 3b, we see that the seasonal variations observed at two hypothetical ground stations separated by 180° appear to be different. Thus, two ground-based observers situated at these locations would infer different inter-annual, annual and semi-annual harmonics even if 24 hour measurements were available to remove tidal effects.

The reason for this is illustrated in Figure 4. It shows the quasi-stationary planetary wave field reconstructed using only the longitude/day-of-year harmonic terms in (1).

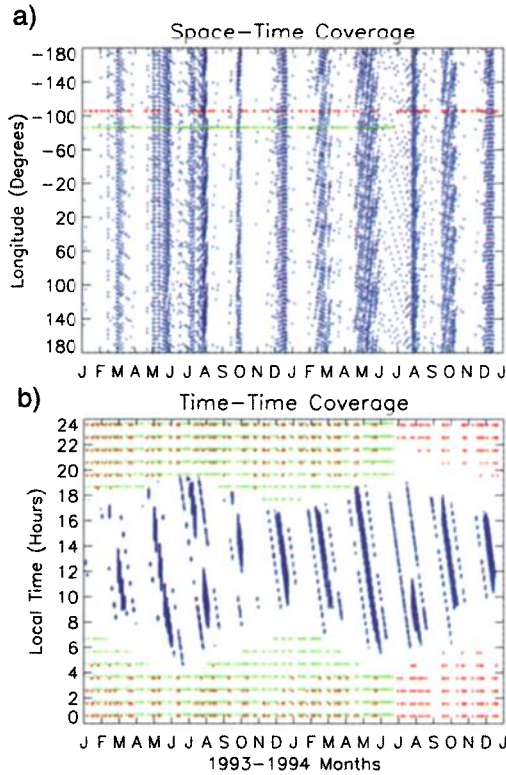


Figure 1. The location of the satellite- and ground-based observations in the space-time (upper) and time-time (lower) domain. The HRDI observations are shown in blue, CSU lidar in red, and PMI in green.

During late 1993 and early 1994 significant stationary longitudinal variations on the order of 8 to 10 K are present.

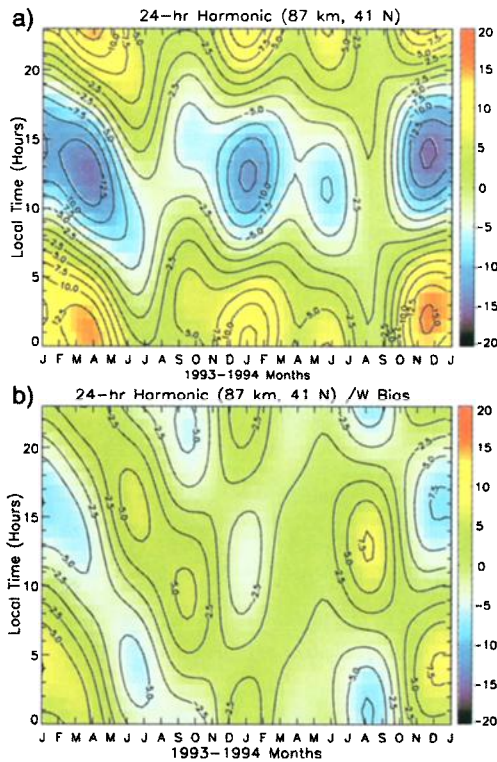


Figure 2. The seasonal variation of the diurnal harmonics in K estimated without (upper panel) and with (lower panel) bias correction factors.

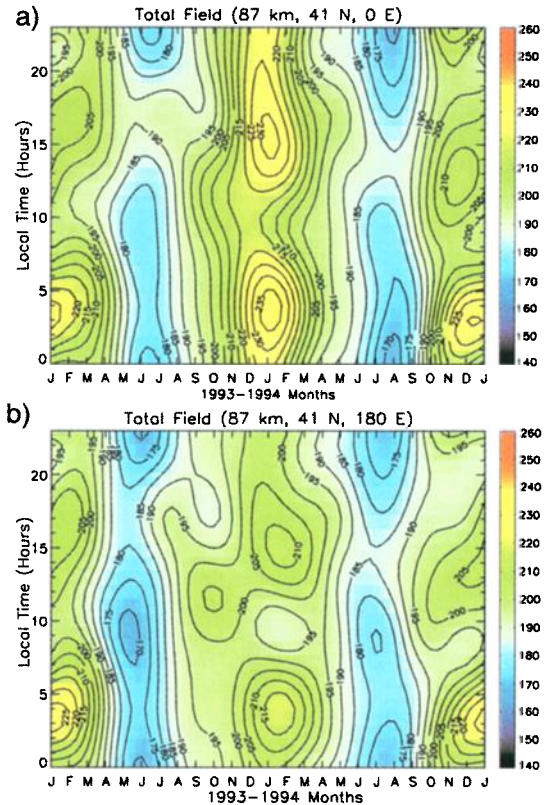


Figure 3. Reconstruction of the mid-latitude 87-km day-of-year/local time temperature surface at 0° E (upper) and 180° E (lower) for 1993 and 1994.

Smith [1997] observed similar planetary-scale waves at these latitudes and heights in HRDI wind data during early 1994 and showed that they are strongly correlated to stationary planetary waves observed at 10 mb (~ 30 km). Figure 4 also shows that stationary planetary waves with amplitudes on the order of 5 K occur during other seasons. The existence of these stationary planetary waves in the data was verified, independent of our fitting analysis, by simply binning the HRDI observations in longitude over a 36-day period. We also noted that longitudinal temperature differences seen in the HRDI data between the CSU and PMI sites were consistent with the longitudinal temperature differences observed

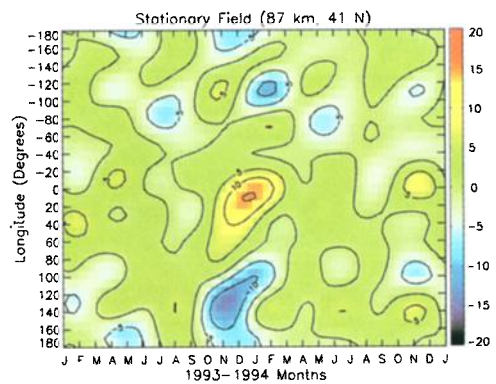


Figure 4. Reconstruction of the mid-latitude stationary wave field at 87 km (day-of-year versus longitude), showing significant quasi-stationary planetary wave variations.

in the ground stations after removing the local time variations and biases.

The annual temperature variation, as well as significant local time variations, can be seen in the temperature fields in Figure 3. Due to the superposition of tidal modes, and in-situ chemical heating, daily local time fluctuations on the order of ± 10 K are observed. The analysis suggests that these variations, longitudinal asymmetries, and instrument biases all play a role in current climatological estimates determined from individual ground- or space-based instruments. For example, after self-consistently accounting for these effects in our inversion, the amplitude of the zonal mean annual harmonic at 87 km is estimated to be 14.1 ± 2.1 K with a phase maximum occurring at 356.2 ± 6.2 days. This amplitude is less than 17.0 ± 2.0 K derived by *She and vonZahn* [1998] using nighttime CSU lidar data and 20.0 ± 0.2 K by *Niciejewski and Killeen* [1995] using PMI data. We also note that this amplitude is significantly greater than the 8 K estimate of *States and Gardner* [2000a] made during the 1996-1998 period using a 24 hour lidar. It is not unreasonable to believe, however, that the amplitude of the annual oscillation at 87 km could vary by as much as ± 5 K on interannual scales.

4. Conclusion

To produce reliable estimates of the spatiotemporal variability of the MLT region we have presented a methodology for combining satellite- and ground-based data sets. It was applied to determine self-consistently the seasonal evolution of the mean state, tides, and stationary planetary waves at 87 km at mid-latitudes to an estimated uncertainty of ± 3 K. Because of calibration biases between the available satellite- and ground-based instruments, we were unable to establish accurately an annual mean temperature (193.5 K) to better than ± 8.5 K. However, by considering the relative variations in the data we resolved spatiotemporal variations in greater detail and accuracy than would have been possible using data from a single instrument.

The derived tidal amplitudes and phases support the results of recent observations and tidal analyses. Further, our results also indicated that in-situ chemical heating may be important. We also observed significant stationary planetary waves in MLT temperatures (amplitudes ~ 10 K). The magnitude of these previously unreported features suggests that they play an important role in the dynamics and energetics of the region. Furthermore, these waves have the potential to alias into climatological estimates of seasonal fluctuations made from single ground stations.

Acknowledgments. Portions of this work were supported by NASA (NGT-51137, NAS5-98045), the Office of Naval Research, and DOE (DE-AI0498AL79800). Observational efforts were supported by NASA (NAS5-27751, NAGI-1315) and NSF (ATM9714676). Devoted efforts of J.R. Yu, M.A. White and S.S. Chen in taking the CSU lidar data are greatly appreciated.

References

Clancy, R. T., D. W. Rusch, and M. T. Callan, Temperature minima in the average thermal structure of the middle mesosphere (70-80 km) from analysis of 40- to 92-km SME global temperature profiles, *Geophys. Res. Lett.*, *99*, 19001, 1994.

- Forbes, J. M., M. Kilpatrick, D. C. Fritts, A. H. Manson, and R. A. Vincent, Zonal mean and tidal dynamics from space: an empirical examination of aliasing and sampling issues, *Ann. Geophys.*, *15*, 1158, 1997.
- Hedin, A. E., Extension of the MSIS thermosphere model into the middle and lower atmosphere, *J. Geophys. Res.*, *96*, 1159, 1991.
- Leblanc, T., I. S. McDermid, and D. A. Ortland, Lidar observations of the middle atmospheric thermal tides and comparison with the High Resolution Doppler Imager and Global Scale Wave Model 2. October observations at Mauna Loa (19.5° N), *J. Geophys. Res.*, *104*, 11931, 1999.
- Melo, S. M., R. P. Lowe, and H. Takahasi, The nocturnal behavior of the hydroxyl airglow at the equatorial and low latitudes as observed by WINDII: Comparison with ground-based measurements, *J. Geophys. Res.*, *104*, 24657, 1999.
- Mlynczak, M. G., and S. Solomon, Middle atmospheric heating by exothermic chemical reactions involving odd-hydrogen species, *Geophys. Res. Lett.*, *18*, 37, 1991.
- Niciejewski, R. J., and T. L. Killeen, Annual and semi-annual temperature oscillations in the upper mesosphere, *Geophys. Res. Lett.*, *22*, 3243, 1995.
- Ortland, D. A., P. B. Hays, W. R. Skinner, and J.-H. Yee, Remote sensing of the mesospheric temperature and O₂(¹Σ) band volume emission rates with the high-resolution Doppler imager, *J. Geophys. Res.*, *103*, 1821, 1998.
- Salby, M. L., Sampling theory for synoptic satellite observations. Part I: Space-Time Spectra, Resolution and Aliasing, *J. Atmos. Sci.*, *39*, 2577, 1982.
- She, C. Y., and U. von Zahn, Concept of a two-level mesopause: Support through new lidar observations, *Geophys. Res. Lett.*, *103*, 5855, 1998.
- She, C. Y. and R. P. Lowe, Seasonal temperature variations in the mesopause region at mid-latitude: comparison of lidar and hydroxyl rotational temperatures using WINDII/UARS OH Height profiles, *J. Atmos. Terr. Phys.*, *60*, 1573, 1998.
- Smith, A. K., Stationary planetary waves in upper mesospheric winds, *J. Atmos. Sci.*, *54*, 2129, 1997.
- States, R. J. and C. S. Gardner, Influence of the diurnal tide and thermospheric heat sources on the formation of mesospheric temperature inversion layers, *Geophys. Res. Lett.*, *25*, 1483, 1998.
- States, R. J. and C. S. Gardner, Thermal structure of the mesopause region (80-105 km) at 40° N latitude. Part I: Seasonal variations, *J. Atmos. Sci.*, *57*, 66, 2000a.
- States, R. J. and C. S. Gardner, Thermal structure of the mesopause region (80-105 km) at 40° N latitude. Part II: Diurnal variations, *J. Atmos. Sci.*, *57*, 78, 2000b.
- Williams, B. P., C. Y. She, and R. G. Roble, Seasonal climatology of the nighttime tidal perturbation of temperature in the midlatitude mesopause region, *Geophys. Res. Lett.*, *25*, 3301, 1998.
- Wunsch, C. *The ocean circulation inverse problem*, 329 pp., Cambridge University Press, New York, New York, 1996.
- Yee, J. H., G. Crowley, R. G. Roble, W. R. Skinner, M. D. Burrage, P. B. Hays, Global simulations and observations of O(¹S), O₂(¹Σ) and OH mesospheric nightglow emissions, *J. Geophys. Res.*, *102*, 19949, 1997.

D. P. Drob, J. M. Picone, S. D. Eckermann, Code 7640, Naval Research Laboratory, 4555 Overlook Ave, Washington, DC 20375. (e-mail: drob@uap.nrl.navy.mil)

C. Y. She, Department of Physics, Colorado State University, Fort Collins, Colorado 80523.

R. J. Niciejewski, J. F. Kalkalidis, D. A. Ortland¹, T. L. Killeen, Space Physics Research Laboratory, The University of Michigan, 2455 Hayward Ave, Ann Arbor, MI 48109.

(Received May 28, 1999; revised June 27, 1999; accepted December 2, 1999)